Acta Crystallographica Section D
Biological Crystallography
ISSN 0907-4449

Low-salt crystallization of T7 RNA polymerase: a first step towards the transcription bubble complex

Chun Jung Chen,[a,b] Zhi-Jie Liu,[a] John P. Rose[a] and Bi-Cheng Wang[a]*

[a]Department of Biochemistry and Molecular Biology, University of Georgia, Athens GA 30602, USA, and [b]Department of Crystallography, University of Pittsburgh, Pittsburgh, PA 15260, USA

Correspondence e-mail: wang@bcl1.bmb.uga.edu

Received 8 December 1998
Accepted 23 March 1999

DNA-dependent RNA polymerase is the key enzyme responsible for the biosynthesis of RNA, a process known as transcription. This process, which decodes the genetic information from DNA, is one of the most significant events in a biological system. The crystallization of both native and a chimeric T7/T3 RNAP using high-salt conditions has been reported previously but these conditions proved unsuitable for DNA–RNAP complex formation since at high-salt concentrations the DNA binding affinity to RNAP is reduced. A search for low-salt crystallization conditions has yielded new low-salt crystals of native T7-RNAP, a chimeric T7-RNAP (T7/T3 RNAP) which contains the T3 promoter recognition sequence, and a T7-RNAP containing an N-terminal histidine tag. The crystals, which are better suited for DNA–RNAP complex formation, belong to space group $P3_121$ with a = 136, c = 156 Å, contain a single molecule per asymmetric unit and diffract to 2.7 Å resolution. Packing analysis shows that the new low-salt crystals have packing contacts similar to those observed in the high-salt T7-RNAP crystals reported previously. The diffraction anisotropicity observed in crystals of T7 RNAP is explained in term of crystal packing.

1. Introduction

The flow of genetic information from DNA to protein is a two-step process, with RNA as an intermediate. The enzyme responsible for catalyzing the synthesis of RNA from DNA is RNA polymerase (RNAP). One of the most studied RNAPs is T7 RNA polymerase (T7-RNAP), a small single-chain DNA-dependent RNAP isolated bacteriophage T7, a virulent bacteriophage which infects *Escherichia coli* (Demerec & Fano, 1945). Despite its simplicity, T7-RNAP is capable of carrying out all steps of the transcription cycle, without the need of auxiliary factors required by the larger multi-subunit polymerases for accurate initiation and termination. T7-RNAP carries out promoter recognition, initiates the RNA chain *de novo*, extends the chain, and finally terminates and is released from the template. Therefore, T7-RNAP provides an excellent system with which to probe the basic mechanism of transcription.

T7-RNAP has been cloned, overexpressed in bacteria (Studier & Dunn, 1983), crystallized (Sousa *et al.*, 1989), and a preliminary model has been published at 3.3 Å resolution (Sousa *et al.*, 1993). However, the crystals, which yielded the published structure, were grown using high salt concentrations (50% ammonium sulfate), conditions that are not optimal for DNA–RNAP complex formation since at high salt concentrations the DNA binding affinity to RNAP is reduced. A search for crystallization conditions using low-salt buffer systems has produced a new crystal form of T7-RNAP. These

Table 1
Data collection and processing statistics.

Crystal	T7LS	T7/T3	HIST7
Molecular weight (Da)	98856	98947	100358
Beamline	NSLS X8C	NSLS X8C	NSLS X8C
Detector	MAR 345	MAR 345	MAR 345
Temperature (K)	100	100	100
Wavelength (Å)	1.0720	1.0720	1.0720
Number of crystals used	3	3	1
Crystal dimensions (mm)	0.2 × 0.2 × 0.8	0.1 × 0.1 × 0.8	0.2 × 0.2 × 0.8
Crystal-to-detector distance (mm)	260	260	260
Rotation for each exposure (°)	1	1	1
Time for each exposure (s)	20	20	60
Total rotation range (°)	180	180	150
Maximum resolution of data (Å)	2.7	2.7	3.1
Number of observations	272898	242594	161845
Number of possible reflections	48033	48066	31984
Number of unique reflections	43854	43788	29361
Number of unique $2\sigma_1$ reflections	41005	40863	27957
$R_{\rm merge}$	0.111	0.120	0.107
Cell constants (Å)			
a	135.0	136.9	138.3
c	155.6	156.2	157.5
Space group	$P3_121$	$P3_121$	$P3_121$

conditions are better suited to DNA complex formation, which is the first step in our goal of the crystallization of the RNAP RNA/DNA transcription elongation complex. We report here the crystallization and preliminary crystallographic analysis of three new low-salt crystal forms of T7 RNA polymerase: native T7-RNAP, a chimeric T7-RNAP (T7/T3 RNAP) which contains the T3 promoter recognition sequence, and a T7-RNAP containing an N-terminal histidine tag (HIST7 RNAP) which will be used for mutation studies.

2. Methods and procedures

2.1. Sample preparation

Both T7-RNAP and the T7/T3-RNAP chimeric protein were prepared as described previously (Davanloo *et al.*, 1984; Sousa *et al.*, 1989, 1990). Samples of HIST7-RNAP were prepared by cloning the coding region of T7-RNAP into a bacterial expression vector containing an N-terminal 6x-histidine tag, pTrcHisA (Invitrogen). The cDNA for T7-RNAP was PCR amplified using a sense primer complementary to the 5′ end of the cDNA and containing an *Nhe*I site for cloning purposes (5′ **GCTAGC** AACACGATTAACATGGC 3′; the *Nhe*I site is in bold and the sequence complementary to the T7-RNAP is underlined). The anti-sense primer for the PCR reaction contained the 3′ end of cDNA, including the stop codon, and a *Hin*dIII site for cloning purposes (5′ G**AAGCTT**TTACGCGAACGCGAAGTC 3′; the *Hin*dIII site is in bold and the sequence complementary to the T7-RNAP is underlined). The template for the PCR reaction was pAR1219. The resulting PCR product was subcloned into pGEM-T vector (Promega) to facilitate restriction digestion of the ends, and then subcloned into pTrcHisA (Invitrogen) using the *Nhe*I and *Hin*dIII sites. The resulting plasmid was named pTrcT7. The sequence of the cloned T7RNAP was confirmed by the Molecular Genetics Instrumentation Facility (MGIF) at the University of Georgia.

For expression of HIST7-RNAP, a 1 l culture of Circlegrow (Bio101, Inc) containing 100 µg ml^{-1} ampicillin was inoculated with *E. coli* JM109 harboring the expression plasmid. The culture was grown at 310 K for 18–20 h with shaking. The cells were then harvested by centrifugation (5000*g*) at 277 K for 20 min. The cell pellet was resuspended in 60 ml of a resuspension buffer containing 30 m*M* Tris–HCl, pH 8.0, 200 m*M* NaCl, 10% glycerol, 0.1 m*M* phenylmethylsulfonyl fluoride (PMSF), and for purification of the holoenzyme, trypsin inhibitor (20 mg/60 ml) was included to prevent proteolysis. The resuspended cells were then sonicated four times (30 s each) on ice, and centrifuged at 44 000*g* at 277 K for 1 h to separate the soluble protein from the cell debris. The soluble protein fraction was passed through a column containing Ni–NTA (Qiagen) resin which was pre-equilibrated with 50 ml of resuspension buffer. The column was washed with 15 ml of resuspension buffer, and then the purified protein was eluted in 10 ml of elution buffer containing 30 m*M* Tris– HCl, pH 8.0, 100 m*M* NaCl, 10% glycerol, 0.1 m*M* PMSF, and 100 m*M* imidazole. The yield of the protein was approximately 10 mg l^{-1} and the purity was better than 95% as assessed by SDS–PAGE and UV–visible spectra.

2.2. Crystallization

Screenings for low salt T7-RNAP crystallization conditions were carried out at 291 K using sitting-drop vapor diffusion. The initial set of low-salt conditions were derived from the Hampton Crystal Screen I with some local modifications. From the initial screen, only solutions containing PEG 8000 produced crystals (microneedles). These conditions were then refined until crystals (T7LS) suitable for X-ray diffraction analysis were obtained. The best crystals (0.2 × 0.2 × 1.0 mm), were grown from 4 µl sitting drops containing equal volumes of protein concentrate (10 mg ml^{-1}) and a reservoir solution, consisting of 50% glycerol, 18% PEG 8000 in 0.1 m*M* HEPES buffer, pH 8.0 which was allowed to equilibrate against 400 µl of reservoir solution for a period of 2–3 weeks.

A similar approach was used for the T7/T3- and HIST7-RNAP crystallization trials. Crystals of T7/T3-RNAP (T7/T3) were grown to a size of 0.1 × 0.1 × 1.0 mm by equilibrating 8 µl sitting drops [containing equal volumes of protein concentrate (10 mg ml^{-1}) and reservoir solution] against 400 µl of reservoir solution, containing 20% glycerol, 24% PEG 8000, 0.2 *M* CsCl in 0.1 *M* sodium phosphate buffer, pH

Table 2
Data-collection statistics for the T7LS crystals.

Resolution		Linear		
D_{max} (Å)	D_{min} (Å)	$\langle I \rangle$	R_{sym}†	Completeness (%)
99.00	5.81	9984.0	0.053	98.4
5.81	4.61	4914.0	0.072	99.3
4.61	4.03	5152.8	0.093	99.0
4.03	3.66	4177.0	0.132	99.2
3.66	3.40	3157.0	0.176	98.4
3.40	3.20	2668.2	0.206	97.2
3.20	3.03	2306.3	0.225	95.1
3.03	2.90	2034.0	0.254	91.1
2.90	2.79	2050.0	0.274	80.9
2.79	2.69	2236.5	0.279	53.0
All data		4051.5	0.111	91.3

† $R_{sym} = \sum(|I - \langle I \rangle|)/\sum(I)$.

Table 3
Data-collection statistics for the T7/T3 crystals.

Resolution		Linear		
D_{max} (Å)	D_{min} (Å)	$\langle I \rangle$	R_{sym}	Completeness (%)
99.00	5.81	5834.3	0.042	98.3
5.81	4.61	3052.8	0.074	99.0
4.61	4.03	3295.7	0.094	98.7
4.03	3.66	2754.4	0.137	98.9
3.66	3.40	2147.5	0.188	98.2
3.40	3.19	1845.0	0.226	97.2
3.19	3.03	1633.4	0.244	95.1
3.03	2.90	1473.4	0.270	91.1
2.90	2.79	1517.8	0.270	80.9
2.79	2.69	1689.6	0.276	52.9
All data		2621.8	0.120	91.1

Table 4
Data-collection statistics for the HIST7 crystals.

Resolution		Linear		
D_{max} (Å)	D_{min} (Å)	$\langle I \rangle$	R_{sym}	Completeness (%)
99.00	6.68	4138.3	0.044	96.2
6.68	5.30	1597.5	0.082	95.4
5.30	4.63	1969.1	0.084	96.4
4.63	4.21	2073.8	0.099	94.8
4.21	3.91	2011.2	0.122	94.7
3.91	3.68	1842.5	0.145	93.4
3.68	3.49	1620.0	0.198	91.8
3.49	3.34	1477.1	0.212	90.0
3.34	3.21	1448.4	0.222	85.1
3.21	3.10	1298.5	0.250	80.2
All data		1985.9	0.107	91.8

8.0, for 2–3 weeks. Crystals of HIST7-RNAP (HIST7) were grown to a size of 0.2 × 0.2 × 0.8 mm in 2–3 weeks using 10 µl sitting drops [containing equal volumes of protein solution (10 mg ml^{-1}) and a reservoir solution] equilibrated against 400 µl of reservoir solution, containing 50% glycerol, 20% PEG 8000 in 0.1 *M* sodium phosphate buffer pH 8.5.

2.3. Data collection

Data for the T7LS, T7/T3 and HIST7 crystals were collected on cryo-cooled crystals (Hope, 1988; Teng, 1990) using a MAR 345 image-plate scanner, beamline X8C, National Synchrotron Light Source (NSLS), Brookhaven National Laboratory. The data were indexed, integrated and scaled using *HKL* 1.9.1 (Otwinowski & Minor, 1997). A summary of data collection and processing parameters for the T7LS, T7/T3 and HIST7 crystals are given in Table 1. For the T7LS and T7/T3 crystals, three 180° data sets were collected on different crystals and scaled together (Otwinowski & Minor, 1997) to give the final data set (see Tables 2 and 3). Because of time constraints, only a single data set was collected on the HIST7 crystals (see Table 4).

2.4. Molecular-replacement calculations

AMoRe (Navaza, 1994) was used for the molecular-replacement calculations. The refined T7HS structure (Protein Data Bank entry 3rnp) was used as the search model. The rotation search was carried out using data in the range of 15–3.5 Å resolution and a Patterson radius of 32 Å. For the T7LS data, the rotation search gave a single solution at $\alpha = 78.67$, $\beta = 87.60$ and $\gamma = 119.25°$ with a correlation coefficient of 23.3 (the next highest solution had a correlation coefficient of 11.8). The translation search yielded a single solution in space group $P3_121$ with $Tx = 0.6215$, $Ty = 0.2230$ and $Tz = 0.1565$. This solution gave a correlation coefficient of 42.5 and an *R* factor of 43.9, the next highest solution had a correlation coefficient of 19.5 and an *R* factor of 50.0. The T7/T3 and HIST7 data gave similar results.

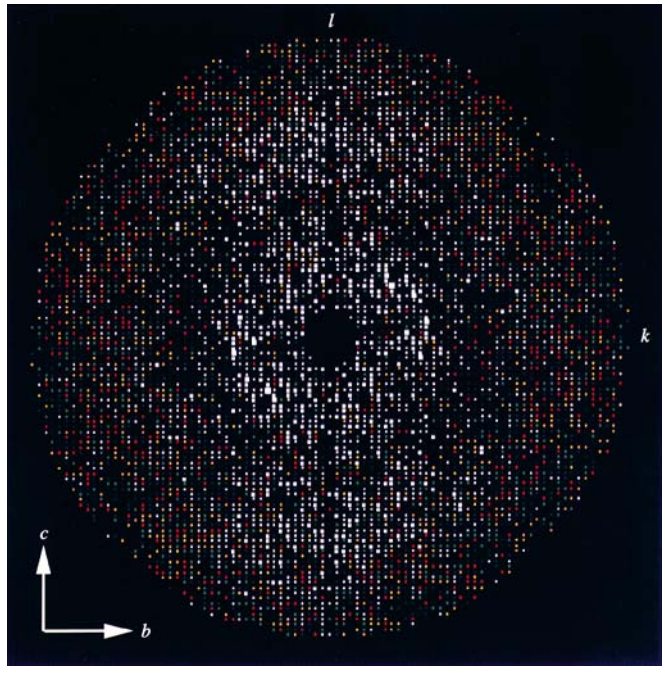

Figure 1
A simulated precession photograph (*PRECESS*, Furey & Swaminathan, 1997) for the *hk*0 layer showing the anisotropic nature of the T7LS diffraction pattern where reflections recorded along the 001 direction are systematically stronger than reflections recorded normal to it. The anisotropic nature of the diffraction pattern can be explained by the crystal packing, which is tighter along the 001 direction.

3. Results and discussion

The T7LS, T7/T3 and HIST7 crystals all grow as long rods with typical dimensions of 0.15 × 0.15 × 0.8 mm. The diffraction patterns for the T7LS, T7/T3 and HIST7 crystals are highly anisotropic with reflections recorded normal to the long axis of the crystal having systematically weaker intensities (see Fig. 1). This phenomenon is also observed in the diffraction pattern of the high salt T7 RNAP crystals (T7HS) reported previously (Sousa *et al.*, 1989, 1993), which also grow as long rods. The T7/T3 crystals appear to diffract better than the crystals of the orthorhombic T7/T3 crystal form reported earlier (Sousa *et al.*, 1990) which were grown under high salt conditions.

The T7LS, T7/T3 and HIST7 crystals appear to be isomorphous since the data sets for the different crystals all indexed in a primitive trigonal lattice with similar unit cell constants (see Table 1). In addition, analysis of the three-dimensional diffraction patterns [*XPREP* (Sheldrick, 1991)] indicated that the space group (systematic absences $000l$, $l \neq 3n$) for these crystals is either $P3_121$ or $P3_221$. Based on one molecule per asymmetric unit (from our molecular-replacement analysis), the Matthews coefficient (Matthews, 1968) is calculated to be a 4.14 Å^3 Da^{-1} which corresponds to a calculated solvent content of 70%. In contrast, the T7HS crystals have a primitive monoclinic lattice, space group $P2_1$ with a = 111.9, b = 137.3, c = 122.1 Å, β = 96.4°, contain three molecules per asymmetric unit and have a calculated solvent content of 61%.

In the T7HS crystals, the three T7-RNAP molecules in the asymmetric unit are related by a non-crystallographic 3_1 screw axis at ψ = 88.9 and φ = 129.4° [*X-PLOR* (Brünger, 1990) convention] which corresponds to the [101] direction, the long dimension of the T7HS crystal. Interestingly, the low salt T7-RNAP crystals possess crystallographic 3_1 screw axis which also corresponds to the long dimension (001 direction) of the low salt crystals. Since both crystal forms exhibit 3_1 screw symmetry, a molecular-packing analysis was carried out to determine if the two crystal forms had similar packing environments (only results for the T7LS crystals will be presented).

The results of the packing analysis are shown in Fig. 2. In the high salt crystals, the non-crystallographic 3_1-screw related molecules appear to form molecular helices running along [101] direction in the crystal while in the low salt crystals, the

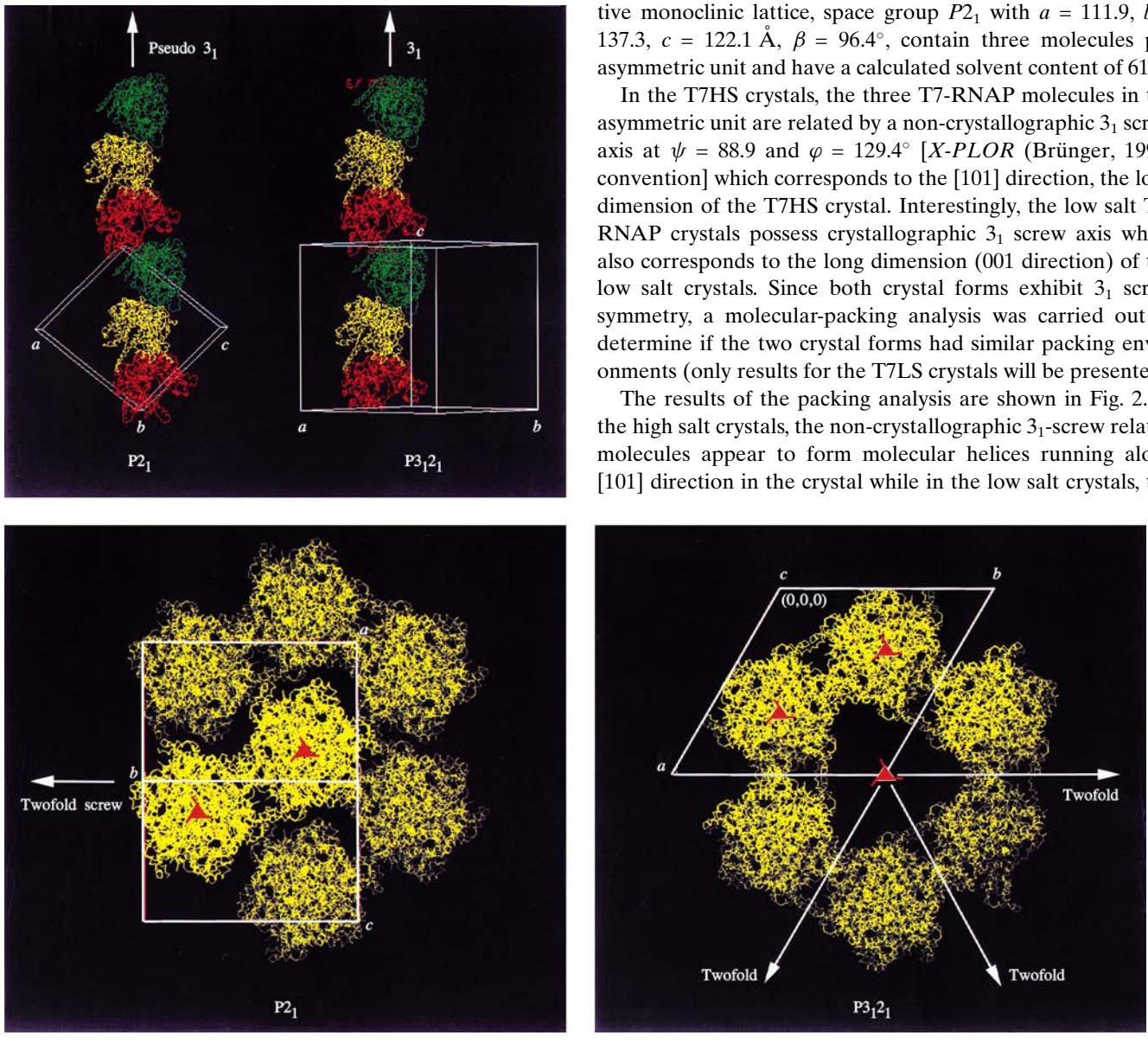

Figure 2
(Top) Molecular packing diagrams for the T7HS (left) and T7LS (right) crystals viewed normal to the 3_1-screw axis. The T7HS crystal form, space group $P2_1$, contains three molecules (colored red, yellow and green) per asymmetric unit which are related by a pseudo 3_1 screw axis running in the 101 direction. The T7LS crystal form, space group $P3_121$, contains only one molecule per asymmetric unit but has a similar molecular packing arrangement along the crystallographic 3_1-screw (001) direction. The corresponding molecules in three asymmetric units of the low salt crystals are given the same color. (Bottom) Molecular packing diagrams for the T7HS and T7LS crystals viewed down the 3_1-screw axis. The low-salt crystal form (right) has large solvent channels running along the c direction. These channels are occupied by T7-RNAP molecules in the high-salt crystal form (left).

crystallographic 3_1-screw axis generates similar molecular helices running along [001] direction in the crystal. In addition, the intra-molecular contacts between molecules related by the 3_1-screw axis are nearly identical in both crystal forms and appear unaffected by the presence or absence of salts. Thus, the similar mode of crystal packing observed along the 3_1-screw direction may explain why both crystal forms grow as long thin needles.

Normal to the 3_1-screw direction, both crystal forms exhibit a similar packing arrangement. However, a large solvent channel running parallel to the *c* axis is observed in low-salt crystal form. This channel is not present in the T7HS crystals where a T7-RNAP molecule is observed to occupy this space. This difference would explain why the T7HS crystals have a lower solvent content (61%) than the 70% solvent content calculated for the low-salt crystals. In addition, compared with the packing contacts observed along the 3_1-screw direction, the intra-molecular packing contacts normal to the 3_1-screw direction are less extensive in both the high- and low-salt crystal forms.

T7-RNAP is both a large and flexible molecule as required by its enzymatic function. The intra-molecular packing contacts observed along the 3_1 axis would tend to stabilize the structure in this direction while the lack of stabilizing packing contacts normal to the 3_1 axis would allow the structure more flexibility (less order) in this region. Thus, the crystals will show more order (better diffraction) along the 3_1 axis and less order (weaker diffraction) normal to it which we believe is the cause of the diffraction anisotropicity observed for both the T7HS and low-salt crystals. Refinement of the low-salt structures is in progress.

The authors wish to thank Ms Tamura Dailey for her help in the preparation of the His-tagged protein, Dr Ming Liu for his help in the preparation of the T7/T3 chimera and Dr M. Gary Newton for his helpful discussions concerning the manuscript. This work was supported by a grant GM41936 from the National Institutes of Health and funds from the Georgia Research Alliance to BCW.

References

Brünger, A. T. (1990). *Acta Cryst.* A**46**, 546–593.
Davanloo, P. A. H., Rosenberg, A. H., Dunn, J. J. & Studier, F. W. (1984). *Proc. Natl Acad. Sci. USA*, **81**(7), 2035–2039.
Demerec, M. & Fano, U. (1945). *Genetics*, **30**, 119–128.
Furey & Swaminathan, (1997). *Methods Enzymol*. **277**, 590–620.
Hope, H. (1988). *Acta Cryst.* B**44**, 22–26.
Matthews, B. W. (1968). *J. Mol. Biol.* **33**, 491–497.
Navaza, J. (1994). *Acta Cryst.* **50**, 157–163.
Otwinowski, Z. & Minor, W. (1997). *Methods Enzymol.* **276**, 307–326.
Sheldrick, G. (1991). *XPREP*. Space group determination and reciprocal space plots. Siemens Analytical X-ray Instruments, Madison, WI, USA.
Sousa, R., Chung, Y. J., McAllister, W. T., Wang, B. C. & Lafer, E. M. (1990). *J. Biol Chem.* **265**, 21430–21432.
Sousa, R., Chung, Y. J., Rose, J. P. & Wang, B. C. (1993). *Nature (London)*, **364**, 593–599.
Sousa, R., Rose, J. P., Lafer, E. M. & Wang, B. C. (1989). *Proteins*, **5**, 266–270.
Studier, F. W. & Dunn, J. J. (1983). *Cold Spring Harb. Symp. Quant. Biol.* **47**(2), 999–1007.
Teng, T. Y. (1990). *J. Appl. Cryst.* **23**, 387–391.